

Surface-enhanced Raman spectroscopy (SERS): nonlocal limitations

G. Toscano,¹ S. Raza,^{1,2} S. Xiao,¹ M. Wubs,¹ A.-P. Jauho,³ S.I. Bozhevolnyi,⁴ and N.A. Mortensen¹

¹Department of Photonics Engineering, Technical University of Denmark, DK-2800 Kgs. Lyngby, Denmark

²Center for Electron Nanoscopy, Technical University of Denmark, DK-2800 Kgs. Lyngby, Denmark

³Department of Micro and Nanotechnology, Technical University of Denmark, DK-2800 Kgs. Lyngby, Denmark

⁴Institute of Sensors, Signals and Electrotechnics, University of Southern Denmark, DK-5230 Odense, Denmark

Compiled October 15, 2018

Giant field enhancement and field singularities are a natural consequence of the commonly employed local-response framework. We show that a more general nonlocal treatment of the plasmonic response leads to new and possibly fundamental limitations on field enhancement with important consequences for our understanding of SERS. The intrinsic length scale of the electron gas serves to smear out assumed field singularities, leaving the SERS enhancement factor finite even for geometries with infinitely sharp features. For silver nano-groove structures, mimicked by periodic arrays of half-cylinders (up to 120 nm in radius), we find no enhancement factors exceeding ten orders of magnitude (10^{10}). © 2018 Optical Society of America

While the Raman response of (bio-)molecules is inherently weak, nanostructures may be used to tailor and tremendously enhance the light-matter interactions. This is the key electromagnetic element of surface-enhanced Raman spectroscopy (SERS) [1]. In particular, metallic nanostructures [2] are known to support plasmonic field-enhancement phenomena which are beneficial for SERS [3]. In many cases, field singularities arise in geometries with abrupt changes in the surface topography. While such singularities constitute the basic electromagnetic mechanism behind SERS, the singularities are on the other hand an inherent consequence of the common local-response approximation (LRA) of the plasmons [4]. In this Letter, we relax this approximation and allow for nonlocal dynamics of the plasmons. To illustrate the consequences we revisit the model geometry in 1, initially put forward by García-Vidal and Pendry [5] to qualitatively explain the electromagnetic origin of the large enhancement factors observed experimentally. The metallic surface topography is composed of a periodic structure of infinitely long metallic half-

cylinders of radius R , resting shoulder-by-shoulder on a semi-infinite metal film. The steep trenches or grooves support localized-surface plasmon resonances (LSPR). Near the bottom of the groove the surfaces of the two touching half-cylinders become tangential to each other and a field singularity forms within the traditional LRA of the dielectric function. In the common treatment, the field enhancement thus eventually turns infinite [6] while it remains finite, albeit large, in any experiment reported so far. Geometrical smoothening is known to remove the singularity within the LRA and in quantitative numerical studies a rounding needs to be added to make numerical convergence feasible [7, 8]. Thus, within the LRA framework the field enhancement would just grow without bound the sharper one could make the geometry confining the plasmon oscillations. Nonlocal effects have been shown to result in large blueshifts and considerably reduced field enhancements (as compared to a local description) in conical tips [9], metallic dimers involving small gaps below a few nanometers [10, 11], or even vanishing gaps [12]. *What is the limit in field enhancements that can be achieved with (geometrically) ideal structures?* This question is important not only from the fundamental but also from applied perspective, as the answer to it would allow one to determine technological tolerances in fabrication of nanostructures designed for achieving record-high field enhancements. In this Letter we show how nonlocal response introduces a new intrinsic length scale that serves to remove the field singularities, leaving field enhancements finite even in geometries with arbitrarily sharp changes in the surface topography. For the particular geometry of Fig. 1 we evaluate $\gamma(\mathbf{r}, \omega) = |\mathbf{E}(\mathbf{r}, \omega)|^4 / |\mathbf{E}_0(\omega)|^4$ and find no (surface averaged) SERS enhancement factors $\langle \gamma \rangle$ exceeding ten orders of magnitude.

The electromagnetic response of a metal is commonly divided into intraband contributions [13] and the dispersive Drude free-electron response $\varepsilon_D(\omega) = 1 + i\frac{\sigma}{\varepsilon_0\omega} = 1 - \frac{\omega_p^2}{\omega(\omega + i/\tau_D)}$, where σ is the complex conductivity also

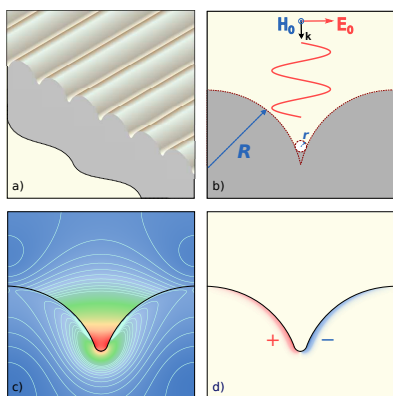


Fig. 1. (a) Groove structure formed by an infinite periodic array of half-cylindrical nanorods. (b) Cross section of the unit cell. (c) and (d) Typical electric-field intensity and charge distributions for a dipole mode.

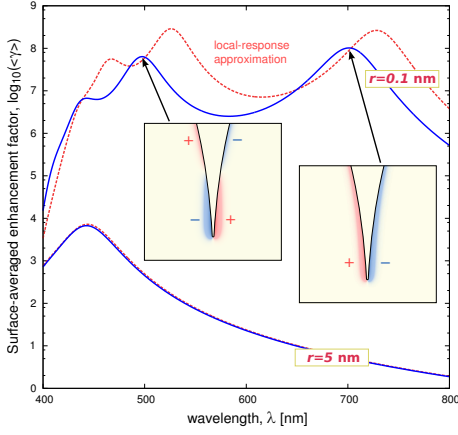


Fig. 2. Surface-averaged SERS enhancement factor $\langle \gamma \rangle$ for the case of $R = 75$ nm with $r = 0.1$ nm (upper curves) and $r = 5$ nm (lower curves). For comparison, the dashed lines show the results of the commonly employed local-response approximation.

appearing in Ohm's law $\mathbf{J} = \sigma \mathbf{E}$. We relax the latter local-response constitutive equation and turn to a linearized hydrodynamic nonlocal treatment [10, 11, 14, 15] where the usual Maxwell wave equation is coupled to a hydrodynamic equation for the current density, see Ref. [11] for the full details of our numerical approach. This is the simplest non-trivial extension of the common LRA Drude model, which in addition to the usual metal parameters (ω_p , τ_D , etc.) now also carries information about the kinetics of the charge carriers at the Fermi level. The strength of the nonlocal correction to Ohm's law depends on the Fermi velocity v_F which introduces a new length scale, being a factor v_F/c of the free-space wavelength $\lambda = 2\pi c/\omega$. For the noble metals, v_F/c is of the order 10^{-2} which explains the overall success of the LRA. However, when exploiting plasmonics at the true nanoscale, effects due to the nonlocal dynamics start to manifest themselves. Field-enhancement structures turn out to be prime examples of this.

We consider the metallic groove structure shown in Fig. 1 which has previously been considered as a model system to mimic corrugated metal surfaces [5]. Alternatively, it may be viewed as a model for arrays of the more recent groove or channel waveguides [7, 16]. In our numerical study, the structure is excited by an incoming plane wave $\mathbf{E}_0(\omega)$, normal to the substrate and with the field polarized perpendicularly to the axis of the half-cylinders, i.e. across the groove cross section. Noble metals are common choices for plasmonics and in the following we focus our attention on silver [13]. The grooves have been shown to support LSPRs [7] which we have previously explored in the context of SERS, using a LRA and with the necessary addition of geometrical smoothing [8]. To quantify the SERS effect and the consequences of nanoscale spatial dispersion, we solve the nonlocal wave equation numerically [11]. As an example of our results, Fig. 2 shows the spectral dependence

of $\langle \gamma \rangle$ throughout the visible regime for groove structures with $R = 75$ nm and with a radius of curvature of the crevice given by $r = 0.1$ nm. The LSPR at $\lambda = 700$ nm allows the (surface-averaged) Raman rate to be enhanced by a factor of 10^8 . For comparison, the dashed line shows results when treating the plasmonic response within the common LRA. In both cases, the resonant behavior is well pronounced, being caused by interference of the incoming field with the gap surface plasmon mode reflected at the bottom, similarly to that described for V-grooves [16]. As a general fingerprint of nonlocal response, the peak is blueshifted compared to the expectations from a local-response treatment of the problem (this happens due to a decrease in the gap plasmon index caused by nonlocal effects [10]). In this particular case, the LSPR by the common treatment is off by more than 25 nm which illustrates the importance of nonlocal effects for quantitative SERS predictions. Even more importantly, the common LRA is seen to significantly overestimate the enhancement factor; for some wavelengths by more than one order of magnitude. The large quantitative differences between the nonlocal treatment and the traditional LRA are associated with changes in the induced-charge distribution (insets of Fig. 2). In the common treatment, the charge is strictly a surface charge while in the general nonlocal case the intrinsic scale v_F/ω serves to spatially smear out the charge distribution. Effectively, this smearing increases the electric field penetration into metal (silver) and thereby increases the field absorption (ohmic loss) and damping of resonant oscillations. Interpreting the field enhancement in a capacitor picture, the finite thickness of the charge distribution near the surface increases the effective separation (beyond that given by the metal-surface geometry) and consequently the capacitor supports a lower electrical field compared to in

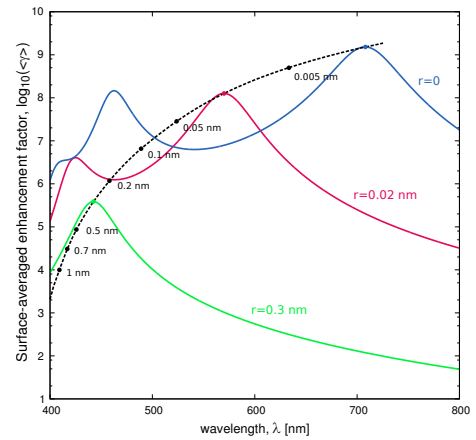


Fig. 3. Surface-averaged SERS enhancement factor $\langle \gamma \rangle$ for the case of $R = 15$ nm and with r varying from 1 nm to 0 nm. The dashed line connecting fundamental dipole resonances for different values of r serves as a guide to the eyes, clearly illustrating both a redshift and the saturation effect in the field enhancement as $r \rightarrow 0$.

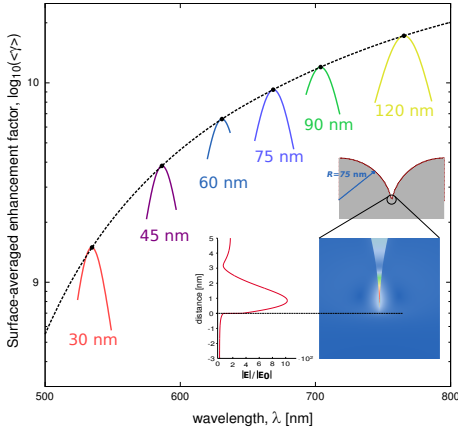


Fig. 4. Near-resonance plots of the surface-averaged SERS enhancement factor $\langle \gamma \rangle$ for arbitrarily well-defined grooves without smoothening ($r = 0$) for six cases with R varying from 30 to 120 nm. The inset shows the field-amplitude distribution $|E|/|E_0|$ for $R = 75$ nm.

the LRA. In general, the intrinsic length scale of the electron gas allows to resolve the field also in the proximity of very sharp corners and tips. On the other hand, by relaxing the sharpness of the trench the influence of spatial dispersion becomes less pronounced, as illustrated in Fig. 2 in the lower set of curves ($r = 5$ nm) where the LRA accounts well for the results obtained from a full nonlocal treatment. We note a drastic change in the field enhancement spectrum, with the fundamental resonance now appearing at around 450 nm, due to a very rapid decrease in the gap plasmon index when the gap width increases (at the groove bottom) from 0.1 to 5 nm.

With less geometrical smoothening (*i.e.* when r is made smaller and smaller) the shortcomings of the LRA become more severe. The LRA anticipates a monotonously increasing enhancement factor [8] and decreasing r also causes a stronger interaction between neighboring half-cylinders and consequently a redshift [5]. Note that in the interpretation based on gap surface plasmons [16], the redshift is simply related to an increase in the gap plasmon index when the gap width decreases at the groove bottom. In Fig. 3 we decrease r from 1 nm down to zero and see how nonlocal effects cause a different trend (indicated by the dashed line) due to the competing length scales. In particular, for $r \lesssim v_F/\omega$ there is a fundamental saturation of the enhancement factor rather than a monotonous increase and for our particular choice of the cylinder radius R we see that the $\langle \gamma \rangle$ does not exceed 2×10^9 .

To explore the ultimate limitations on the SERS in this geometry, Fig. 4 shows results where we have completely refrained from any geometrical smoothening ($r = 0$) and where v_F/ω is the only length scale that puts fundamental limitations on the field enhancement. As the radius R of the half-cylinders is increased from 30 nm to 120 nm we see a redshift of the peak as also anticipated in the LRA [8]. At the same time, the enhancement fac-

tor exhibits an increasing trend where larger cylinders support larger field enhancement by harvesting the incoming field from larger areas. We emphasize that in all examples the field enhancement remains finite despite the fact that the crevice is arbitrarily sharp and well defined ($r = 0$). For the largest radius R considered the electromagnetic SERS enhancement factor does not exceed 2×10^{10} . This illustrates the fundamental limitations imposed by nonlocal response in our specific SERS configuration.

In conclusion, we have shown that a nonlocal treatment of the plasmonic response leads to new and possibly fundamental limitations on the electromagnetic SERS enhancement factor, thereby completely changing the message of the commonly employed local-response approximation of the plasmons. The intrinsic length scale of the electron gas serves to smear out the field singularity that otherwise would arise from a local-response treatment and as a consequence the enhancement remains finite even for geometries with infinitely sharp features. Finally, beyond the linear response fundamental limitations may arise due to nonlinearities [17].

References

1. M. Moskovits, Rev. Mod. Phys. **57**, 783–826 (1985).
2. S. Lal, S. Link, and N. J. Halas, Nature Photonics **1**, 641–648 (2007).
3. K. Kneipp, Phys. Today **60**(11), 40–46 (2007).
4. Y. Luo, J. B. Pendry, and A. Aubry, Nano Lett. **10**, 4186–4191 (2010).
5. F. García-Vidal and J. B. Pendry, Phys. Rev. Lett. **77**, 1183 (1996).
6. I. Romero, J. Aizpurua, G. W. Bryant, and F. J. García de Abajo, Opt. Express **14**, 9988–9999 (2006).
7. E. Moreno, F. J. García-Vidal, S. G. Rodrigo, L. Martín-Moreno, and S. I. Bozhevolnyi, Opt. Lett. **31**, 3447–3449 (2006).
8. S. Xiao, N. A. Mortensen, and A.-P. Jauho, J. Europ. Opt. Soc. Rap. Public. **3**, 08022 (2008).
9. R. Ruppin, Phys. Lett. A **340**, 299–302 (2005).
10. F. J. García de Abajo, J. Phys. Chem. C **112**, 17983–17987 (2008).
11. G. Toscano, S. Raza, A.-P. Jauho, N. A. Mortensen, and M. Wubs, Opt. Express **20**, 4176 – 4188 (2012).
12. A. I. Fernández-Domínguez, A. Wiener, F. J. García-Vidal, S. A. Maier, and J. B. Pendry, Phys. Rev. Lett. **108**, 106802 (2012).
13. S. G. Rodrigo, F. García-Vidal, and Martín-Moreno, Phys. Rev. B **77**, 075401 (2008).
14. J. M. Pitarke, V. M. Silkin, E. V. Chulkov, and P. M. Echenique, Rep. Prog. Phys. **70**, 1–87 (2007).
15. S. Raza, G. Toscano, A.-P. Jauho, M. Wubs, and N. A. Mortensen, Phys. Rev. B **84**, 121412(R) (2011).
16. T. Søndergaard, S. I. Bozhevolnyi, J. Beermann, S. M. Novikov, E. Devaux, and T. W. Ebbesen, Nano Lett. **10**, 291–295 (2010).
17. P. Ginzburg, A. Hayat, N. Berkovitch, and M. Orenstein, Opt. Lett. **35**, 1551–1553 (2010).